R67, the Other Dihydrofolate Reductase: Rational Design of an Alternate Active Site Configuration†

Jian Feng, Sumit Goswami, and Elizabeth E. Howell*

Department of Biochemistry, Cellular, & Molecular Biology, University of Tennessee, Knoxville, Tennessee 37996-0840

Received July 23, 2007; Revised Manuscript Received October 12, 2007

ABSTRACT: R67 dihydrofolate reductase (DHFR) bears no sequence or structural homologies with chromosomal DHFRs. The gene for this enzyme produces subunits that are 78 amino acids long, which assemble into a homotetramer possessing 222 symmetry. More recently, a tandem array of four gene copies linked in-frame was constructed, which produces a monomer containing 312 amino acids named Quad3. Asymmetric mutations in Quad3 have also been constructed to probe the role of Q67 and K32 residues in catalysis. This present study mixes and matches mutations to determine if the Q67H mutation, which tightens binding approximately 100-fold to both dihydrofolate (DHF) and NADPH, can help rescue the K32M mutation. While the latter mutation weakens DHF binding over 60-fold, it concurrently increases k_{cat} by a factor of 5. Two Q67H mutations were added to gene copies 1 and 4 in conjunction with the K32M mutation in gene copies 1 and 3. Addition of these Q67H mutations tightens binding 40-fold, and the catalytic efficiency ($k_{cat}/K_{m(DHF)}$) of the resulting protein is similar to that of Quad3. Since these Q67H mutations can mostly compensate for the K32M lesion, K32 must not be necessary for DHF binding. Another multimutant combines the K32M mutation in gene copies 1 and 3 with the Q67H mutation in all gene copies. This mutant is inhibited by DHF but not NADPH, indicating that NADPH binds only to the wild type half of the pore, while DHF can bind to either the wild type or mutant half of the pore. This inhibition pattern contrasts with the mutant containing only the Q67H substitution in all four gene copies, which is severely inhibited by both NADPH and substrate. Since gene duplication and divergence are evolutionary tools for gaining function, these constructs are a first step toward building preferences for NADPH and DHF in each half of the active site pore of this primitive enzyme.

Dihydrofolate reductase (DHFR) is an important enzyme in folate metabolism. This enzyme reduces dihydrofolate (DHF[1]) to tetrahydrofolate (THF) using NADPH as a cofactor. There are two different DHFR variants, the chromosomal enzyme and an R-plasmid encoded, type II enzyme (*1*, *2*). An example of the latter is R67 DHFR. Neither the sequences nor structures of these DHFRs are homologous. Bacterial chromosomal DHFRs are the target of trimethoprim (TMP), an active site directed inhibitor. Drug resistance to TMP was originally noted in the 1970s (*3*−*5*), and one resistance mechanism involves production of R67 DHFR. While this type II DHFR is not a good catalyst, it does not bind TMP well (K_i = 0.15 mM (*6*)), allowing bacterial cell growth (*7*).

R67 DHFR is unusual as it is a homotetramer with a single active site (*8*), as shown in Figure 1. The crystal structure of R67 DHFR shows 222 symmetry, which dictates that NADPH and DHF must share overlapping sites. This model has been experimentally verified by studies that find a total of two molecules can bind, either two cofactors, or two substrates, or one molecule of each (*9*). The first two complexes are nonproductive while the latter leads to product formation. Different cooperativity patterns between the various ligand combinations facilitate product formation. For example, negative cooperativity between two cofactor molecules occurs so that a preference exists for tightly binding one molecule of NADPH (K_ds of 2.5 and 95 μM respectively). Positive cooperativity between substrate molecules occurs, with weak binding of the first molecule, followed by tight binding of the second (K_ds of 250 and 4.4 μM respectively). Positive cooperativity between NADPH and DHF also exists, so a preferred catalytic pathway is predicted with NADPH binding first, followed by DHF, allowing hydride transfer.

R67 DHFR has been described as a primitive enzyme due to the constraints imposed by its 222 symmetry (*2*, *8*). Table 1 lists a number of factors involved in this designation. To break the 222 symmetry, we constructed a tandem array of four DHFR genes which were linked in frame (*10*, *11*). The linker between gene copies was the natural N-terminus. The

† This work was supported by NSF Grant MCB-0445728.

* Corresponding author. Department of Biochemistry, Cell & Molecular Biology, University of Tennessee, Knoxville, TN 37996-0840. Phone: 865-974-4507. Fax: 865-974-6306. E-mail: lzh@utk.edu.

[1] Abbreviations: R67 DHFR, R67 dihydrofolate reductase; DHF, dihydrofolate; NADP(+/H), nicotinamide adenine dinucleotide phosphate (oxidized/reduced); pABA-glu, *p*-aminobenzoylglutamate tail of dihydrofolate/folate; wt, wild-type; MTA buffer, 100 mM Tris, 50 mM MES, 50 mM acetic acid polybuffer; μ, ionic strength; ITC, isothermal titration calorimetry; $K32M_{half}Q67H_{half}$, the mutant in Quad3 possessing K32M and Q67H mutations in gene copy 1, a K32M mutation in gene copy 3 and a Q67H mutation in gene copy 4; $K32M_{half}Q67H_{all}$, the Quad3 mutant where all gene copies contain the Q67H mutation and gene copies 1 and 3 also contain a K32M mutation.

10.1021/bi701455x CCC: $40.75
Published on Web 12/18/2007

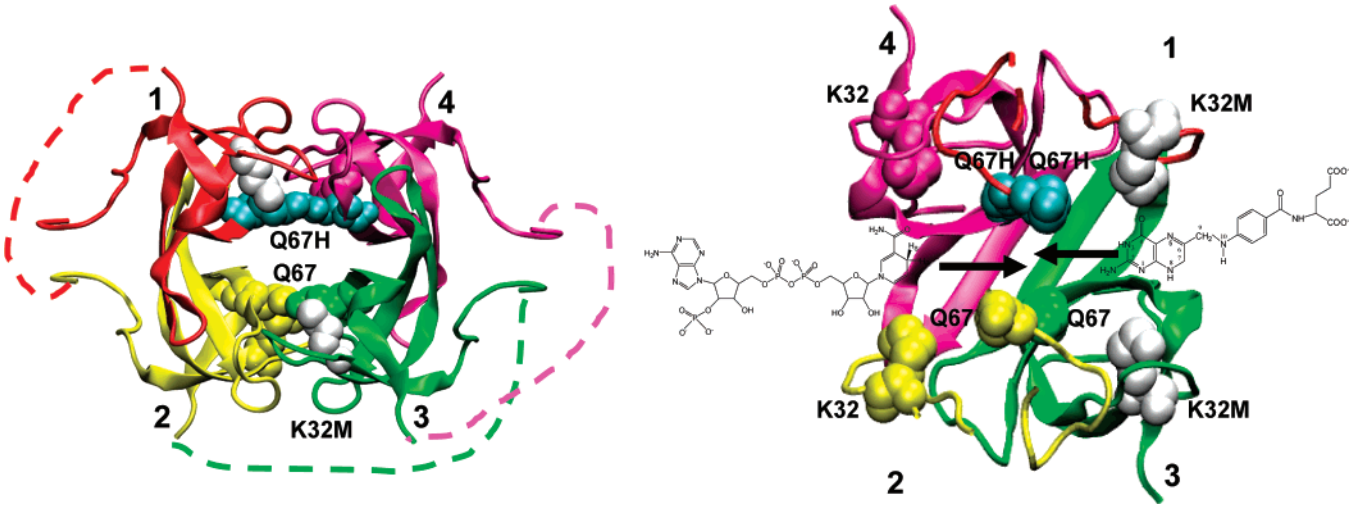

FIGURE 1: The structure of R67 DHFR (1VIE in the Protein Data Bank). Each monomer in wt homotetrameric R67 DHFR is hypothesized to correspond to a domain in Quad3. Monomer 1 is red, monomer 2 is yellow, monomer 3 is green, and monomer 4 is magenta. The left panel shows a ribbon drawing of the homotetramer looking end-on, with the active site pore in the center. The N-termini point to the left and right sides of the image, while the C-termini point up and down. The protein used in this crystal form was obtained by chymotrypsin treatment such that 16 amino acids were cleaved off the N-terminus (*8*, *26*). The expected links between the subunits in R67 DHFR to generate Quad3 are shown as dashed lines. The K32 and Q67 residues are shown using a CPK representation. The expected positions of the K32M:1+3 mutations in Quad3 are shown in white and are pointing toward the viewer. The Q67H:1+4 mutations occur at the top of the active site pore and are colored cyan. The wt K32 and Q67 residues are colored according to the monomer color scheme. The right panel shows a side view of the protein and is related to the left panel by a 90° rotation around the *y*-axis. Part of the protein facing the viewer has been cut away to allow visualization of the pore. Each monomer is labeled 1−4. This panel shows both K32M mutations lying in the same half-pore (right side) and the Q67H mutations at the top of the pore in the center. NADPH is shown entering the wt side of the pore (left), as it prefers to bind first and with specific contacts (*9*, *17*, *20*). Presumably, it will select the tightest binding site available, which in this case is the half pore containing the wt K32 residues. After addition of NADPH, the remaining, K32M mutant half pore is available for DHF, which is shown entering from the right.

Table 1: Factors Involved in Designating R67 DHFR a Primitive Enzyme

Active site challenges?	222 symmetry, 1 active site per homotetramer with a volume of 3626 Å^3 (calculated by CASTp)[a]
Binding site promiscuity?	Each site recognizes both NADPH and DHF,[b] therefore 2DHF and 2NADPH nonproductive complexes can form as well as DHF•NADPH.[c]
Mutational dilemmas?	Four mutations occur per active site and have large effects.[d] For example, the Q67H mutation tightens binding but is accompanied by DHF and NADPH inhibition.[e]
DHF binding conundrum?	*p*-Aminobenzoylglutamate tail of bound DHF is disordered, yet nearby residues affect its binding.[e]
Binding of alternate ligands?	Novobiocin binds more tightly than methotrexate.[f]
Salt effects?	2.5-fold enhancement of k_{cat} in the presence of 0.4 M salt[g]
Conserved acid in active site?	No
Role of water?	Water uptake accompanies DHF binding.[h]
Activation parameters for DHF reduction?	Large entropic component ($T\Delta S^{\ddagger}_{25} = -11.3$ kcal/mol) compared to enthalpy ($\Delta H^{\ddagger}_{25} =$ 6.3 kcal/mol)[i]
Alternate active site sequences? (wild-type sequence is V66-Q67-I68−Y69)	By a directed evolution approach, S66-K67-I68-H69 or I66-N67-R68-Y69 or G66-E67-L68-Y69 are also fully functional.[j]

[a] See http://sts.bioengr.uic.edu/castp/index.php as well as ref (*71*). [b] See refs (*16*, *20*). [c] Described in refs (*9*, *13*, *61*). [d] As per refs (*14*, *15*). [e] See refs (*8*, *18*, *19*). [f] From ref (*53*). [g] See ref (*17*). [h] Unpublished results, Chopra and Howell. [i] From ref (*47*). [j] As per ref (*72*).

resulting protein, Quad1,[2] possessed four times the mass of the R67 monomer and was almost fully active with a 1.6-fold decrease in k_{cat} and a 1.5-fold increase in K_m. Subsequent versions of the Quad1 gene added unique restriction sites between the gene copies to facilitate mutagenesis of the individual gene copies. Also, a S59A mutation was added to gene copy 1 and a H62L mutation to gene copy 4 to produce Quad3 (*11*). These residues occur at the dimer−dimer interfaces in wild type (wt) R67 DHFR. Alone, the S59A or H62L mutations destabilize the homotetramer and favor dimer formation (*12*). Mixed together, they complement each other and reallow tetramer formation. Introduction of these mutations into the tandem gene array was designed to minimize alternate folding topologies (*11*).

Previous mutagenesis studies of the R67 DHFR active site identified K32, V66, Q67, I68, and Y69[3] as the residues most important to binding and catalysis (*13*−*15*). The Q67 residue occurs at the center of the pore and provides a surface for binding of the pteridine ring of DHF and the nicotinamide

[2] The monomer arrangement going counterclockwise in the crystal structure of R67 DHFR (1VIE.pdb) is ABDC. To minimize confusion in the quadruplicated gene construct, we have relabeled the monomers 1234 (=ABCD) going counterclockwise.

[3] The amino acids in the first monomer are labeled 1−78; those in the second monomer, 101−178; those in the third monomer, 201−278; and those in the fourth monomer, 301−378. For brevity, when a single residue is mentioned, all four symmetry-related residues are implied.

ring of cofactor. The Q67H mutation tightens binding of both NADPH and DHF by ~100-fold, but is accompanied by substantial cofactor and DHF inhibition (*13*). A role for Q67 in discriminating between productive and nonproductive (2NADPH and 2DHF) complexes was proposed based on a systematic study of all possible asymmetric mutants in Quad3 (*11*). A double mutant where two Q67H mutations were placed in gene copies 1 and 4 (named Q67H:1+4)[4] shows an intermediate degree of binding tightness and no substrate or cofactor inhibition.

The K32 residue occurs on the edge of the active site pore and forms salt bridges with the 2′phosphate and pyrophosphate moieties of cofactor. K32 has also been proposed to interact with the glutamic acid tail of DHF/folate, either through a direct ionic interaction or through solvent separated ion pairs (*16*−*18*). As all mutants at this position in R67 DHFR resulted in dimers (and were inactive due to loss of the active site pore), the role of K32 was analyzed by salt effects on the steady-state kinetic behavior of the wt and K33M proteins (*17*). A single K32M mutant and three double mutants in Quad3 were also constructed and analyzed (*18*). One double mutant, K32M:1+3, where both mutations are placed on one side of the active site pore (in gene copies 1 and 3), enhances k_{cat} 4−5-fold but greatly weakens binding to DHF.

Since a hallmark of the Q67H mutation is to tighten binding, this present work asks: can introduction of Q67H mutations rescue the binding deficiencies of the K32M:1+3 double mutant yet retain the enhanced k_{cat}? Figure 1 shows the relative positions of the Q67 and K32 residues. Two combinations of mutations were constructed as it was not clear whether two Q67H mutations would be sufficient to tighten binding or whether four Q67H mutations would be needed. The first construct has K32M and Q67H mutations in gene copy 1, a K32M mutation in gene copy 3, and a Q67H mutation in gene copy 4. The second construct has K32M mutations in gene copies 1 and 3, and Q67H mutations in all four gene copies. These two constructs are named $K32M_{half}Q67H_{half}$ and $K32M_{half}Q67H_{all}$ respectively.

Referring again to Figure 1, the simplest model of catalysis in R67 DHFR proposes that DHF occupies half the pore and cofactor the other half. The pteridine ring of DHF and the nicotinamide ring of NADPH encounter each other at the center of the pore where hydride transfer occurs (*16*, *19*, *20*). As described above, a strong preference exists for NADPH to bind first (*9*). Presumably, it will select the tightest binding site available, which in the $K32M_{half}Q67H_{half}$ mutant is the half pore containing the wt K32 residues. Then when DHF binds to this enzyme·NADPH complex, it should be forced into the other half of the pore, which lacks two K32 contacts. The rationale for addition of Q67H mutations is that these residues are proposed to contribute additional stacking interactions with the ring structures of the ligands at the center of the pore (*21*). Q67 residues are ~8 Å distant from K32 side chains, suggesting the potential for additive effects (*22*−*25*). Another consequence of these symmetry breaking mutations may be to begin establishing specificity in each half of the active site pore for NADPH and dihydrofolate.

MATERIALS AND METHODS

Site-Directed Mutagenesis. A tandem array of four R67 DHFR genes was previously constructed where the genes are linked in-frame (*10*, *11*). Mutations were introduced in individual gene copies using the Quikchange kit from Stratagene. The mutant genes were then recloned into the quadruplicated gene. The identities of all four gene copies were verified by DNA sequencing to ensure that no additional mutations occurred.

Protein Purification. Proteins were expressed and purified as previously described (*11*, *26*). Briefly, the *Escherichia coli* strain STBLII (*27*) containing the mutant gene carried by pUC8 was grown in TB media (*28*) with 200 μg of ampicillin/mL at 30 °C for approximately 72 h. 20 μg of TMP/mL was added 48 h after inoculation. Cells were lysed by sonication, and the crude extract was treated with streptomycin sulfate and salted out with 55% ammonium sulfate. Further purification used DEAE Fractogel, Pharmacia MonoQ, and G-75 Sephadex gel filtration columns. The resulting protein was homogeneous as determined by Coomassie Blue staining of SDS−PAGE. Since previous mutants in Quad3 showed a tendency toward aggregation, 0.1 g/L polyethylene glycol (MW 3350) was added to all buffers (*18*, *29*).

Steady-State Kinetics. Steady-state kinetic data were obtained at 30 °C in MTA polybuffer at pH 7.0 using a Perkin-Elmer λ35 spectrophotometer as described elsewhere (*15*). MTA buffer contains 50 mM MES, 100 mM Tris, and 50 mM acetic acid and maintains a constant ionic strength from pH 4.5−9.5 (*30*). The $K32M_{half}Q67H_{half}$ mutant displayed a lag, which was eliminated by preincubation of the enzyme with either NADPH or DHF. The other ligand was then added to initiate the reaction. The concentration of NADPH was held constant at a subsaturating level while the concentration of DHF was varied. This process was repeated using several additional NADPH concentrations. Concentration ranges utilized were 5−77 μM DHF and 13−150 μM NADPH for the $K32M_{half}Q67H_{half}$ mutant and 6−135 μM DHF and 5−174 μM NADPH for the $K32M_{half}Q67H_{all}$ mutant. The data were then fit to an equation describing either the bisubstrate kinetic reaction of DHFR ($K32M_{half}Q67H_{half}$ mutant) or a bisubstrate reaction showing substrate inhibition ($K32M_{half}Q67H_{all}$ mutant) (*11*, *31*). The latter equation is

$$v = (k_{cat}[E_{total}][DHF][NADPH])/((K_{m(NADPH)}K_{d1(DHF)}) + (K_{m(DHF)}[NADPH]) + (K_{m(NADPH)}[DHF]) + ([DHF][NADPH]) + ((K_{m(NADPH)}[DHF]^2)/K_{d2(DHF)})) \quad (1)$$

where v is the velocity of the reaction, $[E_{total}]$, [DHF], and [NADPH] are the concentrations of the enzyme, substrate, and cofactor, respectively, and $K_{d1(DHF)}$ and $K_{d2(DHF)}$ are the first and second binding constants for formation of the

[4] The following system is used to name each of the asymmetric mutants. The residue, residue number, and mutation are listed first, followed by a colon. The asymmetric location of the particular mutations is indicated numerically, where 1 refers to gene copy 1, 2 refers to gene copy 2, etc. For example, the Q67H:1+4 double mutant contains two mutations: glutamine 67 in gene copy 1 has been mutated to histidine, as has glutamine 67 located in gene copy 4. In this mutant, the bottom surface in the active site pore contains two wild-type Gln-67 residues, whereas the top surface of the pore contains two mutant Q67H residues.

Table 2: A Comparison of Steady-State Kinetic Parameters at pH 7.0 for Numerous R67 DHFR Constructs

enzyme	k_{cat} (s^{-1})	NADPH K_m (μM)	DHF K_m (μM)	$k_{cat}/K_{m(NADPH)}$ ($s^{-1}\,M^{-1}$)	$k_{cat}/K_{m(DHF)}$ ($s^{-1}\,M^{-1}$)	any substrate or cofactor inhibition?
Quad3[a]	0.81 ± 0.02	4.4 ± 0.4	6.7 ± 0.4	1.8×10^5	1.2×10^5	no
$K32M_{half}Q67H_{half}$	1.7 ± 0.04	29 ± 2.0	11 ± 0.7	5.7×10^4	1.5×10^5	no
$K32M_{half}Q67H_{all}$	0.49 ± 0.01	9.6 ± 2.8	14 ± 0.9	4.9×10^4	3.5×10^4	yes, DHF
K32M:1+3[b]	≥ 3.7	≥ 150	≥ 400	$\geq 2.6 \times 10^4$	$\geq 9.2 \times 10^3$	no
Q67H:1+4[a]	0.15 ± 0.01	0.95 ± 0.14	2.6 ± 0.5	1.6×10^5	5.8×10^4	no
Q67H:1+2+3+4[a]	0.10 ± 0.01	0.026 ± 0.004	0.13 ± 0.02	3.8×10^6	7.7×10^5	yes, DHF and NADPH
wt R67 DHFR[c]	1.3 ± 0.07	3.0 ± 0.06	5.8 ± 0.02	4.3×10^5	2.2×10^5	no

[a] Values from Smiley et al. (*11*). [b] Values from Hicks et al. (*18*). [c] Values from Reece et al. (*26*).

inhibitory enzyme·2DHF complex. A nonlinear, global fit using SAS (*11*, *31*) resulted in best fit values for k_{cat} and both K_m values as well as $K_{d1(DHF)}$ and $K_{d2(DHF)}$ values. The SAS macro (NLINEK) is available at http://animalscience.ag.utk.edu/faculty/saxton/software.htm. DHF was prepared by reducing folate as described by Blakley (*32*). NADPH was obtained from Alexis Biochemicals. Concentrations of DHF and NADPH were measured using their respective extinction coefficients, $7.75 \times 10^3\ M^{-1}\ cm^{-1}$ and $6.22 \times 10^3\ M^{-1}\ cm^{-1}$ (*33*) at 340 nm. When high concentrations of both DHF and NADPH were used, concentrations were monitored at 360 nm using extinction coefficients of $6.32 \times 10^3\ mol^{-1}\ cm^{-1}$ and $2.94 \times 10^3\ mol^{-1}\ cm^{-1}$ respectively. For reactions monitored at 340 and 360 nm, the extinction coefficients were 12.3×10^3 and $6.32 \times 10^3\ mol^{-1}\ cm^{-1}$ respectively (*34*). Ionic strength (μ) effects were monitored by addition of NaCl to TE buffer (10 mM Tris + 1 mM EDTA) at pH 7.0.

The activities of the mutants were also assessed as a function of pH. Saturating concentrations of NADPH and DHF ($10-20 \times K_m$) were used to monitor activities of Quad3 and the $K32M_{half}Q67H_{half}$ mutant at various pHs. pH profiles of R67 DHFR and its mutants typically display nonunitary slopes, thus data for Quad3 were fit to

$$\log k_{cat} = \log k_{cat\,max} - \log(1 + \chi_1^{\,pH-pK_a} + \chi_2^{\,pK_b-pH}) \quad (2)$$

where $k_{cat\,max}$ is the pH independent rate, pK_a and pK_b are the negative logs of the ionization constants, and χ_1 and χ_2 are the slopes for the acidic and basic titrations. χ values of 10 and 8 represent slopes of 1 and 0.8, respectively (*35*, *36*). Data for the $K32M_{half}Q67H_{half}$ mutant were fit to a standard bell shaped profile. The slope of the acidic titration was varied and the best fit evaluated by adjusted R^2 values. Due to DHF inhibition, this approach was not feasible for the $K32M_{half}Q67H_{all}$ mutant. Here, the maximum rate at different concentrations of DHF was noted. This concentration ($\sim 2\times$ the DHF K_m) was then used to monitor activity at alternate pH values.

The additivity of the mutations was assessed using the following equation:

$$\Delta\Delta G = -RT \ln\left(\frac{k_{cat}/K_m\ (\text{mutant})}{k_{cat}/K_m\ (\text{Quad3})}\right) \quad (3)$$

where R is the gas constant and T is the temperature in K (*23*).

Fluorescence Quenching. Binding affinities were determined by monitoring the effect of ligands on the intrinsic protein fluorescence, as described elsewhere (*37*). Briefly, ligand was added in small aliquots to 2 μM protein in MTA buffer (pH 7). Fluorescence quenching was monitored using a Perkin-Elmer LS-50B fluorimeter. Data were fit to

$$Fl = F_o - 0.5F_o[P_{tot} + K_d + L_{tot} - ((P_{tot} + K_d + L_{tot})^2 - 4P_{tot}L_{tot})^{1/2}] \quad (4)$$

where Fl is the observed fluorescence, L_{tot} is the total ligand concentration, and P_{tot}, K_d and F_o are variables describing the number of enzyme binding sites, dissociation constant and fluorescence yield per unit concentration of enzyme, respectively (*37*).

Isothermal Titration Calorimetry. Dissociation constants and the enthalpy changes associated with binding were monitored using isothermal titration calorimetry (ITC) as previously described (*9*, *38*). A VP-ITC instrument from MicroCal was used and the measurements were performed at 28 °C. The protein concentration in the cuvette ranged from 58 to 150 μM, while the ligand concentration in the injection syringe was ≥ 2.5 mM.

Gel Filtration. Gel filtration was carried out at room temperature using an Agilent 1100 HPLC and an Agilent ZORBAX Bio Series GF-250 gel filtration column equilibrated in 50 mM phosphate buffer (pH 8). The K_{av} values of Quad3 and its mutants ($10-30$ μM protein) were monitored where K_{av} is (elution volume − void volume)/(total bed volume − void volume). The column flow rate was 1 mL/min. A standard curve plotting the molecular weight of protein standards (Pharmacia LMW calibration kit) versus K_{av} allowed determination of the molecular weights of the DHFR variants.

Sedimentation Velocity. Sedimentation velocity experiments were conducted using a Beckman Optima XL-I ultracentrifuge and absorbance optics. Protein samples were dialyzed into 10 mM Tris buffer plus 1 mM EDTA, pH 8 and the dialysate was used as the optical reference. 18 μM protein was loaded (400 μL of loading volume) into double-sector charcoal-filled Epon centerpieces, and sedimentation velocity analysis was carried out at 40,000 rpm at 25 °C using an An50 Ti eight-hole rotor. Sedimentation velocity analysis was performed by direct boundary modeling by using solutions of the Lamm equation and the program Sedfit ((*39*); see www.analyticalultracentrifugation.com). Partial specific volume, buffer density, and viscosity were determined using the software SEDNTERP (John Philo at AMGEN Corp.; see www.jphilo.mailway.com/download.htm).

Circular Dichroism. The conformation of mutants was assessed by circular dichroism (CD) measurements using an AVIV model 202 instrument. Briefly, 5 μM protein in 10 mM phosphate buffer + 1 mM EDTA was scanned at

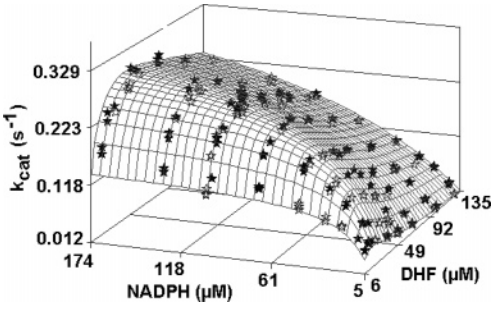

FIGURE 2: Steady-state kinetic data for the $K32M_{half}Q67H_{all}$ mutant. The data were fit to eq 1. Data points above and below the calculated 3D plot are filled and empty stars, respectively. Table 2 gives the best fits for k_{cat} and K_m values. Since DHF inhibition is observed in this mutant, additional terms describing DHF binding to the free enzyme and the enzyme·DHF complex can be obtained and are 18 ± 8 and 8.2 ± 2 μM respectively.

22 °C. At least 10 scans from 190 nm to 300 nm were collected using 1 nm steps and a 2 s integration. An average spectrum was calculated. The CD data were normalized as the mean residue ellipticity by taking 108 g/mol as the mean residue molecular weight (*15*).

RESULTS

Protein Expression and Physical Studies of the Apo Proteins. The $K32M_{half}Q67H_{half}$ and $K32M_{half}Q67H_{all}$ mutants were constructed and expressed. While the yield of soluble, purified protein for the "parent" K32M:1+3 mutant was low (~0.8 mg/L), addition of the Q67H mutations appeared to be stabilizing as expression levels were much higher. Approximately 8 and 20 mg/L yields were obtained for the $K32M_{half}Q67H_{half}$ and $K32M_{half}Q67H_{all}$ mutants respectively.

Since the K32M:1+3 "parent" had a tendency to aggregate, we monitored the oligomeric state of the multimutants using size exclusion chromatography. The molecular weights of Quad3, $K32M_{half}Q67H_{half}$ and $K32M_{half}Q67H_{all}$ were all similar and estimated as 21,700 Da. From the gene sequence, the molecular mass of Quad3 can be calculated as 35,829. There is a difference in the predicted and observed values, with the experimental values being lower than expected. However we note that the mutant and Quad3 values are identical. Since the Agilent GF-250 column can sometimes act as an ion-exchange column (see http://www.chem.agilent.com/cag/Prod/CA/GF250−884972-001.pdf), any retardation of the protein on the column could yield a lower than expected mass. Also aberrant molecular weight estimates determined by gel filtration are not unusual as the shape of the molecule as well as the size affects elution (*40*).

To confirm that the multimutants were monomeric, sedimentation velocity experiments were also performed. The data were fit using a continuous $c(s)$ distribution model (Sedfit (*39*)). The results demonstrate the presence of a single species for the $K32M_{half}Q67H_{half}$ and $K32M_{half}Q67H_{all}$ samples, both displaying an s value of 3.4. For all fits, conversion to a continuous molar mass distribution model demonstrated that both multimutants possess similar molecular mass (36.4 and 40.3 kDa respectively). From the gene sequence, the expected molecular mass is ~35.8 kDa, thus these mutants are monomeric.

To determine whether the protein structure was affected by the mutations, CD spectra were obtained. The spectra at pH 8 and 5 are given in Supporting Information. The signals for the mutants show some differences from those of Quad3. These differences could describe minor alterations in conformation of the proteins and/or alterations in the contribution of aromatic residues to the signal. According to Woody, aromatic residues can contribute significantly to the CD signal (*41*). As K32 is near W38, and Q67 is near W45, the mutations could potentially affect the CD signal. Any conformational changes that might be associated with the mutations are likely to be minimized by addition of one or more ligands, as reasonable enzyme activity levels were observed.

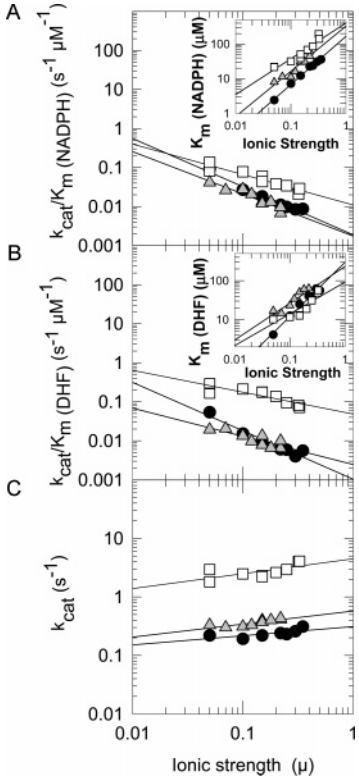

FIGURE 3: Log−log plots of steady-state kinetic values vs ionic strength. Steady-state kinetics were performed with $K32M_{half}Q67H_{half}$ (□) in the presence of increasing NaCl concentrations. Panels A and B show the effects on k_{cat}/K_m with insets showing the effects on the respective K_ms. Panel C shows the effect of increasing salt on k_{cat}. The slopes associated with the plots are given in Supporting Information. Points describing the behavior of the K32M:1+2 (gray filled triangles) and K32M:1+4 (●) mutants are shown for comparison (*18*). These are K32M double mutants where one mutation occurs per half pore, arranged either diagonally or on the same interface respectively. See Figure 1 in Hicks et al. (*18*) for a picture of how the mutations are arranged.

Steady-State Kinetics. The steady-state kinetic behavior of each mutant was analyzed. A lag phase was observed for the $K32M_{half}Q67H_{half}$ mutant if the reaction was initiated by addition of enzyme to a mixture of substrate and cofactor. The lag could be eliminated by preincubation of the enzyme with ligand or substrate. Initial rates were fit to a rate equation describing a bisubstrate mechanism, and the resulting kinetic values are given in Table 2, as well as reference k_{cat} and K_m values for the various "parent" mutants.

When the K_m values for the $K32M_{half}Q67H_{half}$ mutant are compared to those of the K32M:1+3 mutant, it is clear that addition of the Q67H:1+4 mutations has tightened binding. The K_m for DHF has decreased at least 36-fold, while the

Table 3: K_d Values Obtained by Various Techniques

enzyme	complex	K_{d1} (μM)	technique
Quad3	NADPH binary	1.6 ± 0.1	fluorescence, 24 °C, pH 7.0
		4.0 ± 0.3[a]	ITC, 28 °C, pH 8.0
$K32M_{half}Q67H_{half}$	NADPH binary	6.0 ± 0.4	fluorescence, 24 °C, pH 7.0
$K32M_{half}Q67H_{all}$	NADPH binary	2.4 ± 0.2	fluorescence, 24 °C, pH 7.0
		5.0[b]	ITC, 28 °C, pH 8.0
K32M:1+3	NADPH binary	5.2 ± 0.5[c]	fluorescence, 4 °C, pH 7.0
Quad3[a]	DHF binary	$K_{d1} = 46 \pm 0.7$	ITC, 28 °C, pH 8.0
		$K_{d2} = 2.0 \pm 0.2$	
$K32M_{half}Q67H_{all}$	DHF binary	$K_{d1} = 18 \pm 8$	fitting of kinetic data in Figure 2 to eq 1
		$K_{d2} = 8.2 \pm 2.4$	
		Fits to 2 different models gave K_d ranges of 5.4−10.6 μM for both sites.[c]	ITC, 28 °C, pH 8.0
$K32M_{half}Q67H_{all}$	DHF ternary	38 ± 2	ITC, 28 °C, pH 8.0

[a] From Smiley et al. (*11*). [b] See Supporting Information. [c] From Hicks et al. (*18*).

K_m for NADPH has decreased ~5-fold. The approximately 4-fold increase in k_{cat} conferred by the presence of the K32M:1+3 mutations (compared to Quad3) is diminished, but the k_{cat} value for the $K32M_{half}Q67H_{half}$ mutant remains 2-fold higher than that for Quad3.

The further addition of Q67H mutations in gene copies 2 and 3 results in the $K32M_{half}Q67H_{all}$ multimutant. No lag phase was observed for this mutant, however it displayed DHF inhibition, thus a large range of "substrate space" was monitored to allow a good fit. Data for this mutant were fit to eq 1, and a three-dimensional plot of rate vs [DHF] vs [NADPH] is shown in Figure 2. Its kinetic values are also given in Table 2. Since DHF inhibition is observed in this mutant, additional fit values can be obtained describing enzyme + DHF $\rightleftarrows$ enzyme·DHF + DHF $\rightleftarrows$ enzyme·2DHF. These K_d values are 18 ± 8 and 8.2 ± 2.4 μM respectively (also listed in Table 3).

Both k_{cat} and the K_m for NADPH decrease an additional 3-fold in this mutant (over the $K32M_{half}Q67H_{half}$ mutant). While the Q67H:1+2+3+4 mutant displayed substantial cofactor and DHF inhibition (*11*), the $K32M_{half}Q67H_{all}$ multimutant displays only DHF inhibition. Apparently, the K32M:1+3 mutations in this construct still allow binding of a second DHF molecule but prevent binding of a second NADPH molecule. While the $K32M_{half}Q67H_{all}$ mutant does not provide any additional increase in catalytic efficiency over the $K32M_{half}Q67H_{half}$ mutant, it is quite helpful in deciphering how the K32M mutations affect partitioning of NADPH and DHF into each half pore.

Ionic Strength Effects. In a previous study of R67 DHFR, we were interested in how ionic strength (μ) affects binding and catalysis. In the wt homotetramer, addition of salt from $\mu = 0.15$ to 0.42 increases k_{cat} 2.5-fold while concurrently weakening NADPH and DHF binding 5- and 6-fold respectively (*17*). Analyzing the role of K32 via asymmetric mutants found a decreased salt dependence upon removal of two lysine side chains (*18*). Since the K32M:1+3 double mutant could not be saturated with DHF, we were unable to determine its ionic strength dependence. With the addition of the Q67H:1+4 mutations to the K32M:1+3 mutant, we can now probe its ionic strength dependence in the context of this multimutant. Figure 3 shows a log−log plot of the various kinetic parameters vs ionic strength, and the slopes of the various plots are given as a table in Supporting Information. For comparison, data are also shown for the other K32M double mutants (mutations in gene copies 1 and 2 = K32M:1+2 or gene copies 1 and 4 = K32M:1+4). (The ionic strength dependence of the $K32M_{half}Q67H_{all}$ mutant was not determined as fitting yields 5 parameters, which should be confirmed by independent techniques.) In general, the slopes monitoring the salt sensitivities of the $K32M_{half}Q67H_{half}$ mutant are similar to the values for other asymmetric K32M mutants, however these slopes are lower than for wt R67 DHFR, indicating a decrease in ionic strength dependence. We were not expecting a salt dependence for DHF binding to the $K32M_{half}Q67H_{half}$ mutant as in our binding model, DHF interacts with the K32M mutant half of the pore, thus we predicted that its binding would no longer be ionic strength dependent. However a nonzero slope for both $K_{m(DHF)}$ and $k_{cat}/K_{m(DHF)}$ is consistent with interligand cooperativity being quite important in R67 DHFR (*9*, *14*, *15*, *18*). In other words, stacking between the nicotinamide ring of cofactor and the pteridine ring of substrate in the center of the active site pore allows the ligands to "talk" with each other, so perhaps the salt sensitivity of cofactor can be transmitted to DHF. Alternately, K33 residues near the rim of the active site pore have been proposed to help establish a positive electrostatic potential (*16*, *17*) which could still affect k_{on} rates for DHF and thus contribute salt sensitivity toward substrate binding (*42*−*44*).

pH Dependence. Wild-type R67 DHFR is a homotetramer that undergoes a pH dependent dissociation to two dimers. The pH dependence of dissociation arises from protonation of symmetry-related H62 residues that occur at the dimer−dimer interfaces. This process is usually monitored by fluorescence as symmetry-related W38 residues also occur at the two symmetry-related dimer−dimer interfaces. At pH 8, W38 is buried (tetramer), whereas at pH 5 it is exposed to solvent (dimer). Although Quad3 cannot dissociate due to the linker sequences tethering each gene copy product, it can undergo a transition from a "closed" form (active conformation, pH 8) to an "open" form (inactive, pH 4). Previous fluorescence titrations using the Q67H mutant showed a greatly diminished fluorescence signal as well as a decreased tetramer stability (*13*). A low signal change also occurred with the mutants in this study, thus the effects of pH were assessed by monitoring enzyme activity.

Figure 4 shows the pH profile of enzyme activity for Quad3 and the two mutants. A protein concentration dependent acidic pK_a has been previously observed in R67 DHFR which describes loss of activity due to dimer formation (*45*). R67 DHFR does not possess a proton donor,

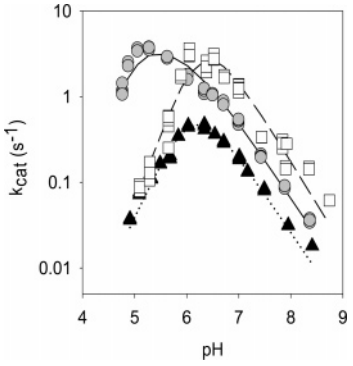

FIGURE 4: pH profiles of k_{cat}. Steady-state kinetics were performed with Quad3 (gray filled circles), $K32M_{half}Q67H_{half}$ (□) and $K32M_{half}Q67H_{all}$ (▲) DHFRs. Each circle and square point corresponds to an initial rate at ligand concentrations which are approximately 20 times the K_m values observed at pH 7.0. Because of substrate inhibition, the triangle points were collected at ~2× the DHF K_m. The theoretical curves were generated by globally fitting the data to eq 2. Best fit values are given in the text.

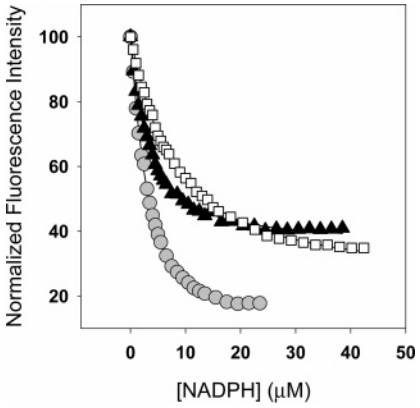

FIGURE 5: Fluorescence quenching of Quad3 and two multimutants by NADPH. The data were normalized to facilitate comparison. The titrations generated for Quad3 (gray filled circles), $K32M_{half}Q67H_{half}$ (□) and $K32M_{half}Q67H_{all}$ (▲) DHFRs are shown. Data were fit to eq 4, and best-fit values are given in Table 3.

and creation of a H62C mutant (where disulfide bonds stabilize the tetramer) results in a monotonic increase in activity as the pH is decreased (*35*). Increased rates have been ascribed to increasing concentrations of protonated, activated DHF (N5 pK_a of free DHF = 2.60 (*46*, *47*)). Thus the basic pK_a in pH profiles of R67 DHFR and Quad3 is only an apparent value. We therefore report solely the acidic pK_a, which describes loss of activity due to formation of an inactive, "open" state. In the pH profile of k_{cat}, a pK_a of 5.1 ± 0.1 is monitored for Quad3 with slopes of 0.8 (basic) and 4 (acidic). This compares to a pK_a of 5.9 for the apo enzyme monitored by fluorescence (*18*). In other words, more acid is required to form open, inactive Quad3 in the presence of ligands (pK_a shift of 0.8 pH unit). The pH independent rate of Quad3 was calculated as 5.4 ± 0.8 s^{-1}.

The activity profile for the $K32M_{half}Q67H_{half}$ mutant displays a different response to pH, indicating that the enzyme is active over a shorter pH range. Calculations yield a pK_a of 6.3 ± 0.2, a pH independent k_{cat} of 7.9 ± 3.2 s^{-1} and slopes of 1 (basic) and 4 (acidic). If binding of DHF and NADPH stabilizes this mutant, the pK_a for the apo enzyme might be expected to be higher. If the pK_a shift is similar to that observed for Quad3 (i.e., 0.8), a pK_a of ~7.1 might be expected for the apo $K32M_{half}Q67H_{half}$ mutant.

With the caveat that the $K32M_{half}Q67H_{all}$ mutant displayed substrate inhibition, the pH profile of this mutant was fit to provide estimates of its behavior. Best fits yield a pK_a of 6.0 ± 0.1, a pH independent k_{cat} of 1.8 ± 0.3 s^{-1} and slopes of 0.8 (basic) and 2 (acidic), indicating a similar pH dependence as the $K32M_{half}Q67H_{half}$ mutant. However a lower k_{cat} is calculated. We additionally note that the Q67H histidine substitutions are apparently not contributing to activity loss as the acidic slopes are similar for Quad3 and the multimutants. Finally, data for the "K32M:1+3 parent" are not available due to the inability to saturate this enzyme with DHF.

Ligand Binding Monitored by Fluorescence and ITC. Since K_m values do not necessarily equal K_d values and can contain kinetic effects, we monitored NADPH binding by fluorescence quenching experiments. Figure 5 shows the titrations, and the resulting K_d values for NADPH are reported in Table 3. The mutants bind NADPH reasonably well, with only 2−4-fold increases in K_d. This result indicates that the binding affinity for NADPH to the wt half of the pore remains mostly unaffected. While the Q67H mutations might be expected to tighten binding (*11*, *13*), loss of a symmetry related binding site due to the K32M mutations could affect κ, the orientational effect in the modified Smoluchowski equation describing diffusion (*18*). For the latter, fewer binding sites would be expected to decrease k_{on} (*48*). We note that the NADPH K_d values are 3−29-fold lower than the observed K_ms, indicating that kinetic terms contribute to the latter. As interligand cooperativity patterns and communication are important in R67 DHFR, one possibility is that if the positioning of DHF is slightly altered in the K32M asymmetric mutants, this information can be imparted to NADPH, which is then reflected in a higher K_m value

Since the protein yields of the multimutants are high, it also became feasible to use ITC to monitor binding. Isotherms for binding in the $K32M_{half}Q67H_{half}$ mutant indicated a substantial enthalpic signal associated with binding of NADPH to enzyme, or DHF to enzyme, or DHF to an enzyme·$NADP^+$ complex. However the protein solutions were cloudy after the titration, thus no quantitative analyses were performed. A parallel experiment injecting buffer into $K32M_{half}Q67H_{half}$ showed small endothermic peaks and resulted in a cloudy solution at the end of the titration, suggesting that the protein tends to aggregate upon stirring.

We were able to perform limited ITC analysis on the $K32M_{half}Q67H_{all}$ mutant. All binding isotherms show exothermic behavior and signals similar to those seen in Quad3 titrations. The NADPH or DHF binary titrations show biphasic behavior, thus curve fitting is not straightforward. Details of the fitting process and sample data sets are given as Supporting Information. In general, the resulting fits agree with the DHF K_d values obtained by fitting of the steady-state kinetic data (Figure 2) and the observed NADPH K_d value obtained via fluorescence quenching.

Preincubation of $K32M_{half}Q67H_{all}$ with $NADP^+$ yielded straightforward titrations upon addition of DHF, suggesting a conformational change upon ligand binding as the origin of the biphasic behavior in the NADPH titrations. Figure 6 shows a ternary complex titration where DHF is injected into a 1:9 mixture of $K32M_{half}Q67H_{all}$·$NADP^+$. Fitting to a single site model yields a stoichiometry of 0.86 ± 0.02, a K_d value

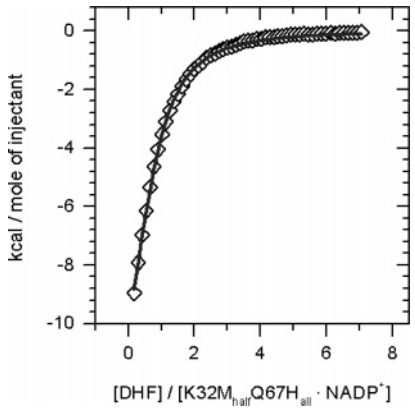

FIGURE 6: Isothermal titration calorimetry analysis of DHF binding to $K32M_{half}Q67H_{all}$ DHFR·$NADP^+$. The protein concentration was 58 μM, and the DHF concentration in the syringe was 2.5 mM DHF. The data were fit using a single site model with best fit values given in Table 3.

of 38 ± 2 μM, and an enthalpy change of −13.7 ± 0.6 kcal/mol (3 experiments). This K_d is ~2-fold higher than the K_m for DHF, perhaps due to structural and electrostatic differences between $NADP^+$ and NADPH or to kinetic effects on K_m. Assuming that $NADP^+$ binds to the half pore containing wt K32 residues and DHF binds to the mutant half pore carrying the K32M mutations, this result clearly indicates that the ionic interaction or solvent separated ion pair between K32 and the glutamate tail of DHF is not the sole source of the enthalpic signal. For comparison, a range of ΔH values (−8.5 to −11.5 kcal/mol) have previously been observed for DHF binding to Quad3·$NADP^+$ as well as various Q67H mutants in complex with $NADP^+$ (*11*).

DISCUSSION

Does NADPH Bind Specifically to the Wt Half of the Active Site Pore? One goal of our mutagenesis of this primitive enzyme is to determine if gene duplication followed by divergence can help increase both binding specificity and catalytic efficiency. From Table 1, it is clear that the 222 symmetry imposes a number of constraints on how the DHFR reaction can be catalyzed. A primary issue is the "one site fits both" approach to binding DHF and NADPH where both ligands must share a site that is not optimized for either.

Prior to optimization, each ligand should show a preference toward binding in a specific half of the active site pore. Using a negative design approach (i.e., blocking of undesired alternatives (*49*−*51*)), a binding site preference for NADPH has been achieved in this study. In the multimutants, NADPH binding is blocked in the half pore containing the K32M mutations such that NADPH only binds to the wt half pore. What evidence exists that NADPH only binds to the wt half of the active site pore? The most compelling data come from the $K32M_{half}Q67H_{all}$ mutant, which does not show NADPH inhibition. This behavior is unlike the Q67H mutant in homotetrameric R67 DHFR or the Q67H:1+2+3+4 mutant in Quad3, which show severe NADPH (and DHF) inhibition (*11*, *13*). In other words, the K32M mutations in one half of the pore prevent NADPH binding and disallow formation of the 2NADPH complex. Other support for NADPH preferring to bind to the wt half pore comes from a comparison of K_{d1} values, where <4-fold differences are seen, compared to Quad3. Another observation predicting that NADPH should strongly prefer the wt half of the pore is the strong salt dependence of NADPH binding, consistent with two ionic interactions between the pyrophosphate bridge and the 2′phosphate and symmetry related K32 residues (*17*). In contrast, addition of salt does not affect the K_d for folate, although a titration in ΔH is observed (*17*).

The above model is also based on an Occam's razor approach, which suggests that the simplest interpretation is preferable. Here, NADPH and DHF do not drastically change their respective binding modes, which show that $NADP^+$ binds tightly using specific contacts, including close contact with K32 residues (*20*, *21*). In contrast, DHF has a disordered tail where the glutamate likely moves back and forth between 2 symmetry related K32s on the rim of the pore and switches between direct and solvent separated ion pairs (*8*, *17*−*19*). The latter binding mode may be more tolerant of the K32M mutation.

Does DHF Bind in the K32M Mutant Half of the Pore? It is clear that DHF must be able to bind in the mutant half of the pore as the $K32M_{half}Q67H_{all}$ mutant shows DHF inhibition, which can only result if both sides of the pore are occupied. Also two molecules of DHF bind to the apo enzyme from ITC titrations. Additionally, DHF binds to both $K32M_{half}Q67H_{half}$·$NADP^+$ and $K32M_{half}Q67H_{all}$·$NADP^+$ as shown by ITC experiments. These binding patterns are consistent with the pABA-glu tail of bound folate/DHF being disordered (*8*, *19*, *20*). Tail flexibility could allow transient or solvent separated ion pair formation with nearby K32 residues. Since solvent separated ion pairs are weaker than direct ionic interactions (*52*), their loss can apparently be tolerated if other compensating interactions are added. The Q67H mutations serve this purpose.

Enthalpy Considerations. Using ITC to monitor formation of either a binary 2DHF complex or the enzyme·$NADP^+$·DHF ternary complex, we were surprised to observe a strong enthalpic signal associated with DHF binding to the multimutants. This result was unexpected as we had previously proposed that an ionic interaction between K32 and the glutamic acid tail of DHF strongly contributed to the ΔH change, since titration of R67 DHFR·$NADP^+$ with dihydrobiopterin, where the pABA-glu tail has been removed, did not yield an enthalpic signal during ITC titrations. (Dihydrobiopterin does bind to wt R67 DHFR with a K_i of ~160 μM (*53*).) The results from these multimutants clearly indicate that the ionic interaction or solvent separated ion pair between K32 and the glutamate tail of DHF cannot be the sole source of the enthalpic signal. Remaining sources contributing to the ΔH change are stacking between nicotinamide and pteridine rings, any differences due to the Q67H mutations and the rest of the binding surface (including A36, Y46, T51, G64, V66, I68 and Y69), and contributions from entrapped water. Previous ITC studies with the Q67H mutant in homotetrameric R67 DHFR as well as asymmetric Q67H mutants in Quad3 show typical enthalpic signals (Q_{total} values of −10 to −12 kcal/mol (*11*, *13*)), so the Q67H mutation does not appear to change ΔH values much. A separate study by Chopra and Howell using osmolytes indicates that water plays a large role in binding DHF (unpublished). Water has also been found to contribute significantly to enthalpy changes in other systems (*54*−*56*), for example Chernevak and Toone found that water reorganization can contribute from 25 to 100% of the binding enthalpy. Also, as noted

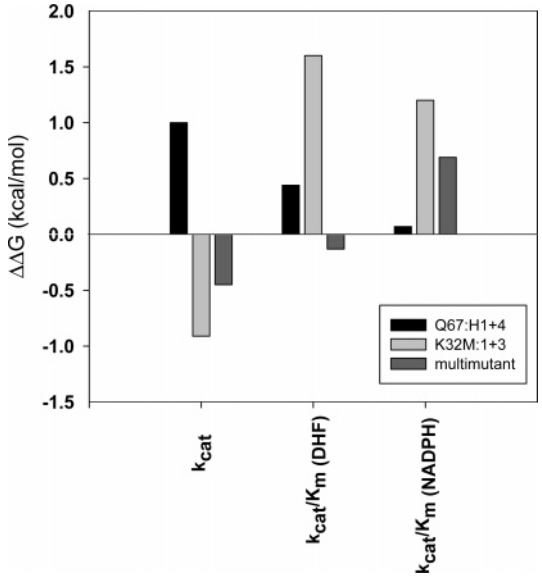

FIGURE 7: Free energy differences calculated based on a double mutant cycle of analysis compared to Quad3 values using eq 4. The comparisons are plotted using black, gray and dark gray bars, respectively, for the K32M:1+3, Q67H:1+4 and $K32M_{half}Q67H_{half}$ mutants. Comparisons are provided for the steady-state kinetic values k_{cat}, $k_{cat}/K_{m(DHF)}$, and $k_{cat}/K_{m(NADPH)}$.

above, increasing the ionic strength of the solution does not affect the K_d for folate, although a titration in ΔH is observed (*17*). Enthalpy−entropy compensation has often been correlated with perturbation of the water network in binding sites (*54*, *57*, *58*). Thus it seems likely that water plays a larger role in the DHF binding enthalpy than previously proposed.

Additivity. The effects of the K32M:1+3 and the Q67H:1+4 mutations on each other were analyzed using a double mutant cycle. A comparison of the various kinetic terms used eq 3. A negative $\Delta\Delta G$ value indicates that the mutant enzyme shows an improved k_{cat}/K_m (or k_{cat} if this is the term compared). The free energy changes associated with the $K32M_{half}Q67H_{half}$ mutant are plotted in Figure 7.

If the mutation has the same effect in two different protein contexts, it is additive. If the effects are different, then the mutations are not additive. Nonadditive effects arise when residues contact each other, when conformational changes in the protein or reorientation of bound substrate occur, and/or when the mechanism or rate-limiting step is altered (*22*−*25*). The Q67H:1+4 mutational pair has a different effect when added to Quad3 compared to K32M:1+3. A coupling energy, ΔG_I, can be calculated using the equation

$$\Delta\Delta G_{multimutant} = \Delta\Delta G_{K32M:1+3} + \Delta\Delta G_{Q67H:1+4} + \Delta G_I \quad (5)$$

where ΔG_I describes the dependence of the mutations on each other or their level of interaction. For k_{cat}, ΔG_I is 0.55 kcal/mol; for $k_{cat}/K_{m(DHF)}$, this term is 2.12 kcal/mol; and for $k_{cat}/K_{m(NADPH)}$, this value equals 0.54 kcal/mol. The mutations do work together, however they are not fully additive. The largest ΔG_I is associated with $k_{cat}/K_{m(DHF)}$, which describes DHF + enzyme·NADPH ⇄ E·DHF·$NADPH^{‡}$, with the latter species describing the transition state. Finding the largest coupling energy associated with $k_{cat}/K_{m(DHF)}$ suggests that DHF binding undergoes the biggest changes, consistent with DHF occupying the mutant half of the pore.

Since the side chain atoms of K32 and Q67 are ∼7−8 Å distant, the coupling energies could derive from slight conformational changes in the protein, reorientation of bound substrate, and/or alteration of the mechanism. As the active site pore is quite voluminous, it is easy to imagine alterations in bound ligand position. Additional effects could arise from alterations in interligand cooperativity.

Necessary and Sufficient. The design process appears to have kept selectivity for NADPH in the half pore that still contains the wt K32 residues. In other words, K32 appears to be necessary and sufficient for NADPH binding. For DHF binding, loss of the K32 residues in the mutant half pore can be compensated for by the Q67H mutations. Here, K32 is sufficient for DHF binding, but not necessary as addition of the Q67H mutations can mostly compensate for loss of the K32 residues. This pattern likely correlates with how the ligands bind. From NMR and crystallography studies, $NADP^+$/(H) is bound with specific contacts, including ionic interactions between the 2′phosphate and the pyrophosphate with symmetry related K32 residues (*19*, *20*, *59*−*61*). In contrast, the *p*-aminobenzoylglutamate (pABA-glu) tail of DHF is disordered by both NMR and crystallography studies (*8*, *19*). The disorder of the pABA-glu tail likely allows transient direct interactions as well as solvent separated ionic interactions with symmetry related K32 residues in Quad3 (*17*, *18*). These interactions are important in binding (as seen in the K32M:1+3 mutant), however they can be eliminated if compensatory mutations are added (i.e., the Q67H mutations).

Enzyme Evolution. In homotetrameric R67 DHFR, the Q67H mutation provides tighter binding to NADPH and DHF at the expense of k_{cat}. In addition, nonproductive complexes readily form as extensive cofactor and substrate inhibition is observed. In contrast, the K32M mutation destabilizes the active tetramer. If K32 function is diminished by increasing salt concentration, then k_{cat} increases while binding to both ligands is weakened. Thus homotetrameric R67 DHFR performs a balancing act, as improvement in one function by addition of a mutation is offset by a decrease in a second function. A compromise between binding and catalysis exists, and increased function is unlikely to evolve in the homotetramer.

According to Ohno, gene duplication creates redundant loci that can accumulate mutations which lead to either loss or gain of function, as long as one of the copies can still perform the required, ancestral task (*62*). In our engineering studies of R67 DHFR, gene quadruplication can allow divergence of individual gene copies. This approach is providing a pathway toward optimizing ligand binding and perhaps increasing function.

Another view of enzyme evolution suggests the presence of a promiscuous intermediate prior to optimization of function (*63*−*65*). Our studies with R67 DHFR support this view. Clearly, R67 DHFR uses a promiscuous surface to bind both substrate and cofactor. This limits its ability to accumulate mutations as a single mutation in four monomers can have large effects on folding, oligomerization state, binding and/or catalysis. Our ability to break the 222 symmetry of the protein using the Quad3 template has led to alternate active site configurations which provide similar levels of function, while blocking formation of the 2NADPH nonproductive complex.

In a recent directed evolution review (*66*), Tao and Cornish state, "Although directed evolution is now used routinely to improve existing enzyme activity, there are still only a handful of examples where substrate selectivity has been modified sufficiently for practical application, and the de novo evolution of function largely eludes us." R67 DHFR is an example of a poor catalyst that has been selected by bacteria to resist the selective pressure of the antibiotic drug, TMP. Its origin is unknown, and it is not a protein scientists would have designed. As such, R67 is helpful as it allows a comparison of catalytic strategies with the well-evolved chromosomal DHFRs (*2*). It can also illustrate simple strategies in catalysis that can be valuable in understanding the basic mechanisms used by other enzymes (*67*). For example, a general hypothesis in enzymology is that increasing levels of preorganization in an enzyme active site lead to enhanced catalytic efficiency (*68*−*70*). R67 achieves some level of preorganization by the initial binding of NADPH in one of four symmetry-related sites. Once bound, NADPH generates a local asymmetry, which in turn favors DHF binding and disfavors binding of a second NADPH molecule. This type of "preorganization" is different from most other enzymes and suggests that ligand−ligand cooperativity plays an important role in R67 catalysis. This view points to negative design (*49*−*51*) being involved in catalytic function. This design element is normally hidden in well-evolved enzymes. As the cooperativity patterns are altered between ligands, as in this study, we hope to determine whether increased specificity and catalytic efficiency result.

ACKNOWLEDGMENT

We thank Cynthia Peterson for critical reading of the manuscript and Nancy Horn for MALDI studies to monitor molecular mass (data not shown).

SUPPORTING INFORMATION AVAILABLE

Figure S1 shows the CD spectra for Quad3 and its mutants. Table S1 lists the slopes of log−log plots of several kinetic parameters versus ionic strength for various mutants compared to wt R67 DHFR. Figure S2 shows a sample titration of NADPH into $K32M_{half}Q67H_{all}$ while Figure S3 shows a sample titration of DHF into this mutant. Details of the fitting process are also given. This material is available free of charge via the Internet at http://pubs.acs.org.

REFERENCES

1. White, P. A., and Rawlinson, W. D. (2001) Current status of the *aadA* and *dfr* gene cassette families, *J. Antimicrob. Chemother. 47*, 495−496.
2. Howell, E. E. (2005) Searching sequence space: two different approaches to dihydrofolate reductase catalysis, *ChemBioChem 6*, 590−600.
3. Amyes, S. G., and Smith, J. T. (1974) R-factor trimethoprim resistance mechanism: an insusceptible target site, *Biochem. Biophys. Res. Commun. 58*, 412−418.
4. Fleming, M. P., Datta, N., and Gruneberg, R. N. (1972) Trimethoprim resistance determined by R factors, *Br. Med. J. 1*, 726−728.
5. Skold, O., and Widh, A. (1974) A new dihydrofolate reductase with low trimethoprim sensitivity induced by an R factor mediating high resistance to trimethoprim, *J. Biol. Chem. 249*, 4324−4325.
6. Amyes, S. G., and Smith, J. T. (1976) The purification and properties of the trimethoprim-resistant dihydrofolate reductase mediated by the R-factor, R388 *Eur. J. Biochem. 61*, 597−603.
7. Taylor, I., Slowiaczek, P., Francis, P., and Tattersall, M. (1982) Purine modulation of methotrexate cytotoxicity in mammalian cell lines, *Cancer Res. 42*, 5159−5164.
8. Narayana, N., Matthews, D. A., Howell, E. E., and Nguyen-huu, X. (1995) A plasmid-encoded dihydrofolate reductase from trimethoprim-resistant bacteria has a novel D2-symmetric active site, *Nat. Struct. Biol. 2*, 1018−1025.
9. Bradrick, T. D., Beechem, J. M., and Howell, E. E. (1996) Unusual binding stoichiometries and cooperativity are observed during binary and ternary complex formation in the single active pore of R67 dihydrofolate reductase, a D_2 symmetric protein, *Biochemistry 35*, 11414−11424.
10. Bradrick, T. D., Shattuck, C., Strader, M. B., Wicker, C., Eisenstein, E., and Howell, E. E. (1996) Redesigning the quaternary structure of R67 dihydrofolate reductase. Creation of an active monomer from a tetrameric protein by quadruplication of the gene, *J. Biol. Chem. 271*, 28031−28037.
11. Smiley, R. D., Stinnett, L. G., Saxton, A. M., and Howell, E. E. (2002) Breaking symmetry: mutations engineered into R67 dihydrofolate reductase, a D2 symmetric homotetramer possessing a single active site pore, *Biochemistry 41*, 15664−15675.
12. Mejean, A., Bodenreider, C., Schuerer, K., and Goldberg, M. E. (2001) Kinetic characterization of the pH-dependent oligomerization of R67 dihydrofolate reductase, *Biochemistry 40*, 8169−8179.
13. Park, H., Bradrick, T. D., and Howell, E. E. (1997) A glutamine 67 to histidine mutation in homotetrameric R67 dihydrofolate reductase results in four mutations per single active site pore and causes substantial substrate and cofactor inhibition, *Protein Eng. Des. Sel. 10*, 1415−1424.
14. Strader, M. B., Chopra, S., Jackson, M., Smiley, R. D., Stinnett, L., Wu, J., and Howell, E. E. (2004) Defining the binding site of homotetrameric R67 dihydrofolate reductase and correlating binding enthalpy with catalysis, *Biochemistry 43*, 7403−7412.
15. Strader, M. B., Smiley, R. D., Stinnett, L. G., VerBerkmoes, N. C., and Howell, E. E. (2001) Role of S65, Q67, I68, and Y69 residues in homotetrameric R67 dihydrofolate reductase, *Biochemistry 40*, 11344−11352.
16. Howell, E. E., Shukla, U., Hicks, S. N., Smiley, R. D., Kuhn, L. A., and Zavodszky, M. I. (2001) One site fits both: a model for the ternary complex of folate + NADPH in R67 dihydrofolate reductase, a D_2 symmetric enzyme, *J. Comput.-Aided Mol. Des. 15*, 1035−1052.
17. Hicks, S. N., Smiley, R. D., Hamilton, J. B., and Howell, E. E. (2003) Role of ionic interactions in ligand binding and catalysis of R67 dihydrofolate reductase, *Biochemistry 42*, 10569−10578.
18. Hicks, S. N., Smiley, R. D., Stinnett, L. G., Minor, K. H., and Howell, E. E. (2004) Role of Lys-32 residues in R67 dihydrofolate reductase probed by asymmetric mutations, *J. Biol. Chem. 279*, 46995−47002.
19. Li, D., Levy, L. A., Gabel, S. A., Lebetkin, M. S., DeRose, E. F., Wall, M. J., Howell, E. E., and London, R. E. (2001) Interligand Overhauser effects in type II dihydrofolate reductase, *Biochemistry 40*, 4242−4252.
20. Krahn, J., Jackson, M., DeRose, E. F., Howell, E. E., and London, R. E. (2007) Crystal structure of a type II dihydrofolate reductase catalytic ternary complex, *Biochemistry*. [Online early access]. DOI: 10.1021/bi701532r. Published Online: Dec 4, 2007. http://pubs.acs.org/cgi-bin/asap.cgi/bichaw/asap/html/bi701532r.html.
21. Divya, N., Grifith, E., and Narayana, N. (2007) Structure of the Q67H mutant of R67 dihydrofolate reductase-NADP+ complex reveals a novel cofactor binding mode, *Protein Sci. 16*, 1063−1068.
22. Wells, J. A. (1990) Additivity of mutational effects in proteins, *Biochemistry 29*, 8509−8517.
23. Carter, P. J., Winter, G., Wilkinson, A. J., and Fersht, A. R. (1984) The use of double mutants to detect structural changes in the active site of the tyrosyl-tRNA synthetase (Bacillus stearothermophilus), *Cell 38*, 835−840.
24. Mildvan, A. S. (2004) Inverse thinking about double mutants of enzymes, *Biochemistry 43*, 14517−14520.
25. Mildvan, A. S., Weber, D. J., and Kuliopulos, A. (1992) Quantitative interpretations of double mutations of enzymes, *Arch. Biochem. Biophys. 294*, 327−340.
26. Reece, L. J., Nichols, R., Ogden, R. C., and Howell, E. E. (1991) Construction of a synthetic gene for an R-plasmid-encoded dihydrofolate reductase and studies on the role of the N-terminus in the protein, *Biochemistry 30*, 10895−10904.

27. Strader, M. B. H., and E. E. (1997) Stable Maintenance of a Tandem Array of Four R67 Dihydrofolate Reductase Genes, *Gibco-BRL Focus 19*, 24−25.
28. Tartof, K., and Hobbs, C. (1987) Improved media for growing plasmid and cosmid clones, *BRL Focus 9*, 12.
29. de Bernandez Clark, E., Schwartz, E., and Rudolph, R. (1999) Inhibition of aggregation side reactions during *in vitro* protein folding, *Methods Enzymol. 309*, 217−235.
30. Ellis, K. J., and Morrison, J. F. (1982) Buffers of constant ionic strength for studying pH-dependent processes, *Methods Enzymol. 87*, 405−426.
31. Smiley, R. D., Saxton, A. M., Jackson, M. J., Hicks, S. N., Stinnett, L. G., and Howell, E. E. (2004) Nonlinear fitting of bisubstrate enzyme kinetic models using SAS computer software: application to R67 dihydrofolate reductase, *Anal. Biochem. 334*, 204−206.
32. Blakley, R. L. (1960) Crystalline Dihydropteroylglutamic Acid, *Nature 188*, 231−232.
33. Horecker, B. L., and Kornberg, A. (1948) The Extinction Coefficients of the Reduced Band of Pyridine Nucleotides, *J. Biol. Chem. 175*, 385−390.
34. Baccanari, D., Phillips, A., Smith, S., Sinski, D., and Burchall, J. (1975) Purification and properties of *Escherichia coli* dihydrofolate reductase, *Biochemistry 14*, 5267−5273.
35. Park, H., Zhuang, P., Nichols, R., and Howell, E. E. (1997) Mechanistic studies of R67 dihydrofolate reductase. Effects of pH and an H62C mutation, *J. Biol. Chem. 272*, 2252−2258.
36. Murphy, D. J., and Benkovic, S. J. (1989) Hydrophobic interactions via mutants of Escherichia coli dihydrofolate reductase: separation of binding and catalysis, *Biochemistry 28*, 3025−3031.
37. Dunn, S. M., Lanigan, T. M., and Howell, E. E. (1990) Dihydrofolate reductase from *Escherichia coli*: probing the role of aspartate-27 and phenylalanine-137 in enzyme conformation and the binding of NADPH, *Biochemistry 29*, 8569−8576.
38. Wiseman, T., Williston, S., Brandts, J. F., and Lin, L. N. (1989) Rapid measurement of binding constants and heats of binding using a new titration calorimeter, *Anal. Biochem. 179*, 131−137.
39. Schuck, P. (2000) Size-distribution analysis of macromolecules by sedimentation velocity ultracentrifugation and lamm equation modeling, *Biophys. J. 78*, 1606−1619.
40. Potschka, M. (1987) Universal calibration of gel permeation chromatography and determination of molecular shape in solution, *Anal. Biochem. 162*, 47−64.
41. Woody, R. W. (1995) Circular dichroism, *Methods Enzymol. 246*, 34−71.
42. Kiel, C., Selzer, T., Shaul, Y., Schreiber, G., and Herrmann, C. (2004) Electrostatically optimized Ras-binding Ral guanine dissociation stimulator mutants increase the rate of association by stabilizing the encounter complex, *Proc. Natl. Acad. Sci. U.S.A. 101*, 9223−9228.
43. Selzer, T., Albeck, S., and Schreiber, G. (2000) Rational design of faster associating and tighter binding protein complexes, *Nat. Struct. Biol. 7*, 537−541.
44. Selzer, T., and Schreiber, G. (2001) New insights into the mechanism of protein-protein association, *Proteins 45*, 190−198.
45. Nichols, R., Weaver, C. D., Eisenstein, E., Blakley, R. L., Appleman, J., Huang, T. H., Huang, F. Y., and Howell, E. E. (1993) Titration of histidine 62 in R67 dihydrofolate reductase is linked to a tetramer to two-dimers equilibrium, *Biochemistry 32*, 1695−1706.
46. Maharaj, G., Selinsky, B. S., Appleman, J. R., Perlman, M., London, R. E., and Blakley, R. L. (1990) Dissociation constants for dihydrofolic acid and dihydrobiopterin and implications for mechanistic models for dihydrofolate reductase, *Biochemistry 29*, 4554−4560.
47. Chopra, S., Lynch, R., Kim, S. H., Jackson, M., and Howell, E. E. (2006) Effects of temperature and viscosity on R67 dihydrofolate reductase catalysis, *Biochemistry 45*, 6596−6605.
48. von Hippel, P. H., and Berg, O. G. (1989) Facilitated target location in biological systems, *J. Biol. Chem. 264*, 675−678.
49. Richardson, J. S., and Richardson, D. C. (2002) Natural beta-sheet proteins use negative design to avoid edge-to-edge aggregation, *Proc. Natl. Acad. Sci. U.S.A. 99*, 2754−2759.
50. Hellinga, H. (1998) Construction of a Blue Copper Analogue through Iterative Rational Protein Design Cycles Demonstrates Principles of Molecular Recognition in Metal Center Formation, *J. Am. Chem. Soc. 120*, 10055−10066.
51. Hecht, M. H., Richardson, J. S., Richardson, D. C., and Ogden, R. C. (1990) De novo design, expression, and characterization of Felix: a four-helix bundle protein of native-like sequence, *Science 249*, 884−891.
52. Levy, Y., and Onuchic, J. N. (2006) Water mediation in protein folding and molecular recognition, *Annu. Rev. Biophys. Biomol. Struct. 35*, 389−415.
53. Jackson, M., Chopra, S., Smiley, R. D., Maynord, P. O., Rosowsky, A., London, R. E., Levy, L., Kalman, T. I., and Howell, E. E. (2005) Calorimetric studies of ligand binding in R67 dihydrofolate reductase, *Biochemistry 44*, 12420−12433.
54. Chervenak, M. C. T., and Eric, J. (1994) A Direct Measure of the Contribution of Solvent Reorganization to the Enthalpy of Binding, *J. Am. Chem. Soc. 116*, 10533−10539.
55. Cooper, A. (2005) Heat capacity effects in protein folding and ligand binding: a re-evaluation of the role of water in biomolecular thermodynamics, *Biophys. Chem. 115*, 89−97.
56. Holdgate, G. A., Tunnicliffe, A., Ward, W. H., Weston, S. A., Rosenbrock, G., Barth, P. T., Taylor, I. W., Pauptit, R. A., and Timms, D. (1997) The entropic penalty of ordered water accounts for weaker binding of the antibiotic novobiocin to a resistant mutant of DNA gyrase: a thermodynamic and crystallographic study, *Biochemistry 36*, 9663−9673.
57. Frisch, C., Schreiber, G., Johnson, C. M., and Fersht, A. R. (1997) Thermodynamics of the interaction of barnase and barstar: changes in free energy versus changes in enthalpy on mutation, *J. Mol. Biol. 267*, 696−706.
58. Dunitz, J. D. (1995) Win some, lose some: enthalpy-entropy compensation in weak intermolecular interactions, *Chem. Biol. 2*, 709−712.
59. Brito, R. M., Reddick, R., Bennett, G. N., Rudolph, F. B., and Rosevear, P. R. (1990) Characterization and stereochemistry of cofactor oxidation by a type II dihydrofolate reductase, *Biochemistry 29*, 9825−9831.
60. Brito, R. M., Rudolph, F. B., and Rosevear, P. R. (1991) Conformation of $NADP^+$ bound to a type II dihydrofolate reductase, *Biochemistry 30*, 1461−1469.
61. Pitcher, W. H., 3rd, DeRose, E. F., Mueller, G. A., Howell, E. E., and London, R. E. (2003) NMR studies of the interaction of a type II dihydrofolate reductase with pyridine nucleotides reveal unexpected phosphatase and reductase activity, *Biochemistry 42*, 11150−11160.
62. Ohno, S. (1970) *Evolution by Gene Duplication*, Springer-Verlag, Berlin.
63. Khersonsky, O., Roodveldt, C., and Tawfik, D. S. (2006) Enzyme promiscuity: evolutionary and mechanistic aspects, *Curr. Opin. Chem. Biol. 10*, 498−508.
64. Jensen, R. A. (1976) Enzyme recruitment in evolution of new function, *Annu. Rev. Microbiol. 30*, 409−425.
65. Matsumura, I., and Ellington, A. D. (2001) In vitro evolution of beta-glucuronidase into a beta-galactosidase proceeds through non-specific intermediates, *J. Mol. Biol. 305*, 331−339.
66. Tao, H., and Cornish, V. W. (2002) Milestones in directed enzyme evolution, *Curr. Opin. Chem. Biol. 6*, 858−864.
67. Alonso, H., and Gready, J. E. (2006) Integron-sequestered dihydrofolate reductase: a recently redeployed enzyme, *Trends Microbiol. 14*, 236−242.
68. Rajagopalan, P. T., and Benkovic, S. J. (2002) Preorganization and protein dynamics in enzyme catalysis, *Chem. Rec. 2*, 24−36.
69. Warshel, A. (1998) Electrostatic origin of the catalytic power of enzymes and the role of preorganized active sites, *J. Biol. Chem. 273*, 27035−27038.
70. Marti, S., Roca, M., Andres, J., Moliner, V., Silla, E., Tunon, I., and Bertran, J. (2004) Theoretical insights in enzyme catalysis, *Chem. Soc. Rev. 33*, 98−107.
71. Liang, J., Edelsbrunner, H., and Woodward, C. (1998) Anatomy of protein pockets and cavities: measurement of binding site geometry and implications for ligand design, *Protein Sci. 7*, 1884−1897.
72. Schmitzer, A. R., Lepine, F., and Pelletier, J. N. (2004) Combinatorial exploration of the catalytic site of a drug-resistant dihydrofolate reductase: creating alternative functional configurations, *Protein Eng. Des. Sel. 17*, 809−819.

BI701455X